

Shaping Self-imaging Bottle Beams with Modified Quasi-Bessel Beams

Li Li,¹ Woei Ming Lee^{2,*} Xiangsheng Xie,¹ Wieslaw Krolikowski,^{3,4} Andrei V. Rode³ and Jianying Zhou^{1,**}

¹The State Key Laboratory of Optoelectronic Materials and Technologies,
Sun Yat-sen University, Guangzhou 510275, China

²Research School of Engineering, Australian National University, Canberra ACT 0200, Australia

³Laser Physics Centre, Research School of Physics and Engineering,
Australian National University, Canberra ACT 0200, Australia,

⁴Texas A&M University at Qatar, Doha, Qatar

*steve.lee@anu.edu.au, **stszjv@mail.sysu.edu.cn

Received Month X, XXXX; revised Month X, XXXX; accepted Month X, XXXX;
posted Month X, XXXX (Doc. ID XXXXX); published Month X, XXXX

Coherent generated of self-imaging bottle beams, typically formed by interfering two coherent Quasi-Bessel beams, possess a periodic array of intensity maxima and minima along their axial direction. In practice, the overall quality of the self-repeating intensity patterns possesses large intensity variations that have yet to be unresolved. In this paper, we increase consistency of intensity of self-imaging bottle beams through a spatial frequency optimization routine. By doing so, we increased the effective length of self-imaging bottle beams by 74%. Further, we show that this approach is applicable to higher-order self-imaging beams which display complex intensity structures. The enhancement in these modified self-imaging beams could play a significant role in optical trapping, imaging and lithography. © 2014 Optical Society of America
OCIS codes: (140.3300) Laser beam shaping; (070.6120) Spatial light modulators; (070.7345) Wave propagation.

Self-imaging phenomenon has been used in a number of applications, such as microscopy imaging [1], lithography [2], and optical manipulation [3, 4]. Talbot effect, a well known optical phenomenon of self-imaging, periodically reproduces transverse intensity patterns along its longitudinal direction. Using iterative numerical algorithms, it is possible to calculate fixed gratings [5] or dynamic holograms [6, 7] tailoring arbitrary self-imaging light fields. The lateral intensity pattern at each longitudinal interval (Talbot's length) undergoes spreading due to diffraction. Hence, these self-imaging patterns do exhibit changes during propagation.

Self-imaging can also be observed in beam shaping using Bessel light fields [8-10] which are also known as self-imaging bottle beams. Such bottle beams, formed by linear superposition of multiple co-propagating Bessel beams, are used in imaging [11], and optical manipulation [4, 12]. In practice, the bottle beams [13, 14] are prone to large intensity variations during propagation, hence limiting their performance. This is primarily because the experimentally formed Bessel beams are typically truncated and an approximate of the ideal Bessel beam. Hence, they are termed as Quasi-Bessel beam (QBB). In order to improve the quality of self-imaging bottle beams, there is a need to shape the axial intensity of the QBBs. Čižmár and Dholakia [15] proposed a spatial frequency optimization approach to control the intensity variation of holographic QBBs. These so-called modified Quasi-Bessel beams (mQBB) possess the axial intensity distribution that can be tailored to a particular practical application.

In this paper, we demonstrate for the first time that the spatial frequency optimization technique can be adapted to increase the effective performance of

self-imaging bottle beams. We quantify the effective performance by means of effective length, which is defined as the full width at half maximum (FWHM) of the axial intensity envelope of the bottle beam. The optimization method enables us to co-propagate two or more modified QBBs of matching intensity distributions, which in turn, produces well-defined alternating intensity along the propagation direction. The effective length of self-imaging sequence was observed to increase by 74% compared to that before optimization. Furthermore, we applied the optimization approach to generate complex intensity structures with higher order mQBBs and interference of multiple mQBBs.

Next, we describe the theoretical and experimental framework used in generating optimal self-imaging bottle beams with a modified mixed-region amplitude freedom (MRAF) method and a spatial light modulator (SLM) respectively. We use SLM to realize the spatial frequency control which has been used in holographic lithography [16] and image restoration [17].

The field distribution of the l^{th} order Bessel beam of the first kind can be expressed as $E_l(r, \phi, z) = AJ_l(k_r r) e^{il\phi} e^{ik_z z}$, where k_r and k_z represent the radial and longitudinal wave vector respectively, and ϕ_l is the azimuthal angle. The intensity distribution of two co-propagating Bessel beams with different axial propagation constants is given by [18]

$$I(r, z, \phi) = J_{l_1}(k_{r_1} r)^2 + J_{l_2}(k_{r_2} r)^2 + 2A' J_{l_1}(k_{r_1} r) J_{l_2}(k_{r_2} r), \quad (1)$$
$$\times \cos[(k_{z_1} - k_{z_2})z + \theta]$$

where A' represents the amplitude factor, and $\theta = \phi_1 - \phi_2$ is a mutual phase. The total light intensity oscillates (cosine term) with propagation, which results in a self-imaged optical bottle beam. Each bottle is represented by a dark spot surrounded by intensity maxima. By changing the propagation constants (kz) of constituent Bessel beam components, the number of bottles can be varied.

For ideal Bessel beams, as described in Eq (1), the transverse intensity distributions are independent of the propagation distance, i.e. the beam maintains a constant central spot intensity and size over an unlimited propagation distance. In practice, the intensity, the axial intensity of the of the QBB has a limited propagation distance where the intensity is constant. Hence, the interference of the QBBs will lead to lower number of optical bottle beams within the same propagation distance, i.e. shorter effective length.

Cizmar and Dholakia [15] identified the optimal relationship between the axial intensity distribution and the spatial frequency content of the beam structure in Fourier space. Using a modified MRAF method, based on the Gerchberg-Saxton (GS) algorithm, the authors optimized the desired spatial frequency contents. The optimized frequency is converted into a kinoform [15, 19-20] to generate a QBB with desired axial profile.

In cylindrical coordinates, the on-axis distribution of an optical field can be linked with its spatial spectrum by a one-dimensional Fourier transform [15],

$$U(r=0, z) = \int_0^k k_z F(\sqrt{k^2 - k_z^2}, z=0) e^{ik_z z} dk_z, \quad (2)$$

where k represents the wave vector, k_z is the longitudinal component of wave vector, and F denotes the spatial spectrum of the field. If we want to construct a QBB with a uniform longitudinal intensity distribution $U(r=0, z) = \exp(ik_{z0}z), |z| \leq z_m$,

where $k_{z0} = \sqrt{k^2 - k_{r0}^2}$ is the axial component of the wave vector, and k_{r0} represents the radius of the ring shaped QBB spectrum, z_m is the maximum uniform length of the desired mQBB. The corresponding spectrum can be obtained by the inverse Fourier transformation of Eq. (2).

Next, we consider an optical bottle formed by the interference of two zero-order QBBs with uniform axial intensity. Its spatial spectrum is given by superposition of the QBB spectra,

$$F_s(k_r, z=0) = \sum_{i=1}^2 \frac{1}{\rho k_z} \frac{\sin[z_m(k_z - k_{zi})]}{k_z - k_{zi}}. \quad (3)$$

When the two QBB components are higher-order

beams with opposite phase factors ($-/+l^{\text{th}}$ order QBB), the transverse intensity pattern of resulting beam will be self-imaged $2l$ petals instead of a ring, and the intensity structure will rotate during propagation [21]. For higher-order QBB,

, the frequency spectrum will contain an infinity which limits the modified MRAF algorithm. To solve this problem, we added the spiral phase only to the kinoform of zero-order modulated QBB. By axial shaping of each higher-order QBB component, the transverse petal-like pattern will maintain a uniform longitudinal intensity. A modified GS algorithm, which will be explained later, is adopted to transform the spectrum into a kinoform. We will show below that by imprinting the kinoform onto the SLM, the bottle beam with uniform axial peak intensity can be easily constructed.

The GS iterative method [19] is a widely used algorithm for phase retrieval. The idea is to carry out fast Fourier transform (FFT) back and forth iteratively between the spectral and the image planes. In each iteration, we retain the phase of the optical field, but replace the intensity with the incident beam pattern and the desired intensity structure in the respective Fourier planes. Although this method is straightforward and easy to implement, the intensity profile formed by the resulting hologram is of rather yields poor holographic reconstruction.

Pasienski and DeMarco proposed MRAF scheme based on the GS algorithm, improving the resulting accuracy by one order of magnitude [20]. In this algorithm the image plane is decomposed into two subsets: the signal region (target image) and the noise region (stray phase and amplitude). The ratio of the light power in signal and noise regions contributes to final image. In each iteration the calculated intensity distribution in the signal region is replaced by the desired structure while the rest of the frequency content is preserved. This scheme leads to excellent computational results for numerous applications, but it is restricted to control of beam pattern in a transverse plane. Cižmár and Dholakia [15] made some further modifications to the MRAF algorithm by simultaneously substituting the phase and amplitude in the signal region, and successfully generalized the method to generate Quasi-Bessel beams.

We applied the modified MRAF algorithm to optical bottle formed by interference of two co-propagating zero-order QBBs with uniform axial intensity distribution. The field at an arbitrary plane perpendicular to the z axis can be formally expressed as

$$E(x, y, z) = F^{-1}\{F[E(x, y, 0)]e^{-ik_z z}\}, \quad \text{where}$$

F and F^{-1} represent the Fourier and inverse Fourier transform, and $E(x, y, 0)$ is the field distribution right after the Fourier lens [22].

Fig.1 shows the simulation results of optical bottle beam without (Fig.1(a)) and with (Fig.1(b)) the

frequency optimization. The transverse propagation constants of two co-propagating QBBs with the same amplitude were $k_{r1} = 0.01k_0$, $k_{r2} = 0.008k_0$ respectively.

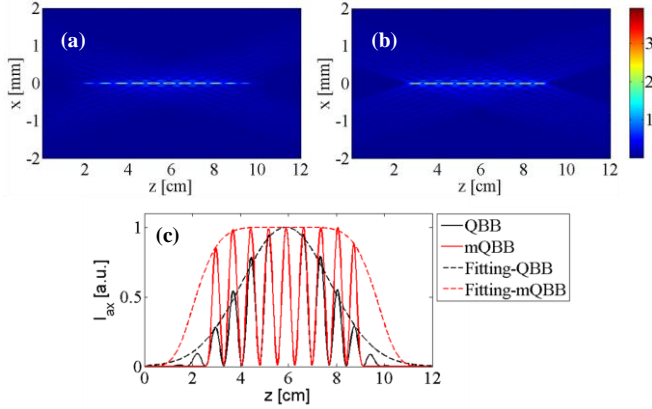


Fig.1 Simulating the propagation of optical bottle beam formed by interfering two co-propagating QBBs. (a) Field distribution of unmodulated bottle beam. (b) Field distribution of modulated bottle beam. (c) On-axis intensity of bottle beam before and after modulation, Gaussian and super-Gaussian fitting are performed respectively to get the effective length (FWHM of the fitting curve). The effective length of bottle beam is increased by 74% after modulation.

It is clearly seen [black line in Fig.1 (c)] that the envelope of the axial intensity exhibits a distinct peak. As a result, the quality of the optical bottles varies with propagation direction. The intensity peaks of the bottles at the both ends are weak and would adversely affect trapping or imaging. Hence, the effective operational length of the beam is significantly reduced. The problem is rectified by using the modulated bottle beam, as shown with red line in Fig.1 (c). Using the spatial frequency optimization technique, the effective length of bottle beam is increased by 74%.

Apart from zero-order QBB, we tested the effectiveness of the optimization method for two co-propagating higher-order QBBs carrying nonzero topological phase. We confirmed that even in such case our technique leads to the uniform axial intensity distribution as depicted in Fig.2. For two QBB with opposing topological charges ± 3 , the resulting beam forms a self-imaging petal structure, as shown in the inset of Fig.2 (a). The pattern rotates around z-axis during propagation even though the total orbital angular momentum is zero. For two QBBs having the same topological charge 3, the resulting transverse intensity pattern exhibits a ring structure with the size of the ring periodically oscillating with propagation, as shown in Fig.2 (b). The simulations show the ability of modified QBB to maintain consistently their quality.

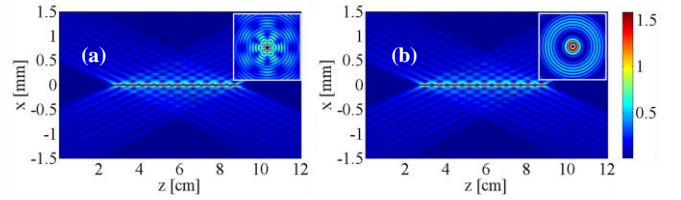


Fig.2 Self-imaging bottle beam generated by the interference of two higher-order QBBs. (a) Two QBB components with the opposing topological charge ± 3 . (b) Two QBB components with the same topological charge 3. The insets show the transverse structure of the beam at $z=6$ cm.

The experimental bottle beam generation and measurement of optical bottle beam with modulated axial intensity is examined. A linearly polarized Gaussian beam at 633 nm was filtered and expanded by a Galilean telescope constructed from a $\times 40$ microscope objective, 20 μ m pinhole and a planar-convex lens ($f=75$ mm). The beam was incident onto the SLM (Holoeye Pluto) chip at an incident angle less than 6° . The Pluto SLM is a reflective phase only device with 1920×1080 resolution and 8 μ m pixel pitch. The SLM with 256 grey levels is calibrated to deliver linear phase modulation up to 2π at 633 nm.

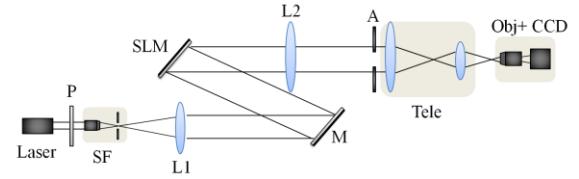


Fig.3 Experimental setup. P: polarizer, SF: spatial filter, M: mirror, A: aperture, Tele: telescope, L1, L2: lenses, Obj : Microscope Objective, CCD: Charge Coupled Device

The optical bottle beam was formed at the back focal plane of L2, see Fig.3, where an aperture is placed to separate the target field from the background. The beam was then compressed with a telescope (Tele) comprising two lenses with focal length 20 cm and 5 cm respectively. An imaging system consisting of a $\times 20$ microscope objective and CCD camera (Mshot MD10), placed on a translation stage with a range of 10cm and minimum resolution of 10 μ m, was designed to characterize the resulting optical field. The translation stage is controlled manually to capture the lateral distribution of the field with a step of 0.2 mm.

The theoretical and experimental results of optical bottle beam without and with optimized modulation are illustrated in Fig.4. To ensure clearer comparison between experiment and theory, the intensity distributions of each data set are normalized to their maximum intensity ($I_{ax} / \max(I_{ax})$). It can be seen that the experimental results agree very well with the simulation previously obtain in Fig.1.

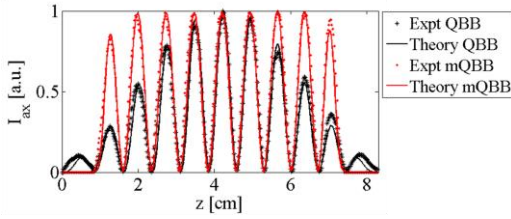


Fig.4 Axial intensity distribution of bottle beam without and with spatial modulation..

It should be stressed that the axial shaping technique discussed here is not restricted to two QBBs interference. In fact, the technique can easily be extended to any number of co-propagating QBBs. As an example we considered an interference of three co-propagating equal amplitude beams. The radial propagation constants of all beams are additional beam has radial propagation constant $k_{r1} = 0.01k_0$, $k_{r2} = 0.008k_0$ and $k_{r3} = 0.009k_0$, respectively. The simulation results and experimental data are depicted in Fig.5. We observe that the presence of the third beam alters the interval and width of each self-repeating bottle beam. This could be useful in optical trapping where the extent of the bottle determines the size of the particles which can be trapped.

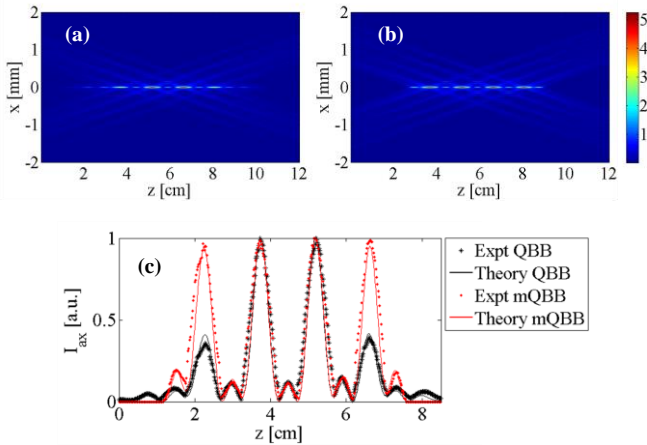


Fig.5 Intensity distribution of beam field formed by three fundamental QBBs without (a) and with (b) spatial modulation.

In summary, we demonstrated and analyzed the generation of self-imaging optical bottle beams via spatial frequency optimization technique. The spatial spectrum of the modulated bottle beam is determined and is transformed to a phase only hologram by using the modified MRAF algorithm. The technique is versatile and can be extended to higher-order QBB and multiple QBB interference. Our experimental results match well with our theoretical prediction. This technique is both flexible and powerful in introducing uniform optical bottles in each self-imaging intervals. Although the method ensures high fidelity of beam shaping it suffers similarly to that used earlier [15] from low diffraction efficiency.

We envisioned that the optimization of these self-imaging optical bottles would prove to be useful in optical trapping, transport and imaging.

This work is financially supported by the State Key Program for Basic Research of China (Grant No. 2012CB921904), the National Natural Science Foundation of China (Grant No. 61205018) and the Fundamental Research Funds for the Central Universities. This work is also supported under Australian Research Council's /Discovery Projects/ funding scheme (project number DP110100975). We also thank Niko Eckerskorn for proof reading the manuscript.

References

1. W. Yashiro, S. Harasse, A. Takeuchi, Y. Suzuki, and A. Momose, *Phys. Rev. A*, **82**, 043822 (2010)
2. A. Isoyan, F. Jiang, Y. C. Cheng, F. Cerrina, P. Wachulak, L. Urbanski, J. Rocca, C. Menoni, and M. Marconi, *J. Vac. Sci. Technol. B*, **27**, 2931, (2009).
3. Y. Y. Sun, J. Bu, L. S. Ong, and X.-C. Yuan, *Appl. Phys. Lett.* **91**, 051101 (2007).
4. T. ěižmár V. Kollárová, Z. Bouchal and P. Zemánek, *New Journal of Physics*, **8**, 1 (2006).
5. W. H. F. Talbot, *Philos. Mag.* **9**, 401 (1836).
6. J. Courtial, G. Whyte, *Opt. Express* **14**, 2108 (2006).
7. S. D. Nicola, P. Ferraro, G. Coppola, A. Finizio, G. Pierattini, and S. Grilli, *Opt. Lett.* **29**, 104, (2004).
8. J. Durnin, J. J. Miceli, Jr., and J. H. Eberly, *Phys. Rev. Lett.* **58**, 1499 (1987).
9. C. A. McQueen, J. Arlt, and K. Dholakia, *Am. J. Phys.* **67**, 912 (1999)
10. Z. Bouchal, J. Wagner, and M. Chlup, *Opt. Commun.* **151**, 207 (1998).
11. G. S. Liu, C. H. Yang, J. G. Wu, *Opt. Eng.* **52**, 091714 (2013).
12. B. P. S. Ahluwalia, X.-C. Yuan and S. H. Tao, *Opt. Express* **12**, 5172, (2004).
13. B. P. S. Ahluwalia, X.-C. Yuan, and S. H. Tao, *Opt. Commun.* **238**, 177 (2004).
14. D. McGloin, G.C. Spalding, H. Melville, W. Sibbett, K. Dholakia, *Opt. Commun.* **225**, 215 (2003).
15. T. Cizmar and K. Dholakia, *Opt. Express*, **17**, 15558 (2009).
16. J. T. Li, Y. K. Liu, X. S. Xie, P. Q. Zhang, B. Liang, L. Yan, J. Y. Zhou, G. Kurizki, D. Jacobs, K. S. Wong, and Y. C. Zhong, *Opt. Express* **16**, 12899 (2008).
17. H. X. He, Y. F. Guan, and J. Y. Zhou, *Opt. Express* **21**, 12539 (2013).
18. S. Chávez-Cerda, M. A. Meneses-Nava, and J. M. Hickmann, *Opt. Lett.* **23**, 1871 (1998).
19. R. W. Gerchberg and W. O. Saxton, *Optik*, **35**, 237, (1972).
20. M. Pasienski and B. DeMarco, *Opt. Express*, **16**, 2176 (2008).
21. R. Vasilyeu, A. Dudley, N. Khilo, and A. Forbe, *Opt. Express*, **17**, 23389 (2009).
22. G. Lifante, *Integrated Photonics: Fundamentals* (John Wiley & Sons, Ltd, Chichester, UK, 2005), Chap. 5.